

# Transient excited-state absorption measurements in chromium-doped forsterite

N. Zhavoronkov

*JV "SOLAR TII," 15/2 F. Skoryna Street, 220067 Minsk, Belarus*

V. Petrov\* and F. Noack

*Max Born Institute for Nonlinear Optics and Ultrafast Spectroscopy, 2A Max-Born-Straße, 12489 Berlin, Germany*

(Received 18 June 1999)

The nonradiative transition dynamics between the excited  ${}^3A''[{}^3E({}^3T_{1a})]$  state and the metastable  ${}^3A''[{}^3E({}^3T_2)]$  storage state of the tetravalent chromium ion ( $\text{Cr}^{4+}$ ) in forsterite is investigated using femto-second excite-and-probe technique. Following excitation to  ${}^3T_{1a}$  with pump pulses at 750 or 773 nm the induced excited state absorption was probed with femtosecond pulses in the ultraviolet (306 nm), visible (650 nm), and infrared (1500 nm). The nonradiative decay time from  ${}^3T_{1a}$  to  ${}^3T_2$  was estimated from the rise time of the excited state absorption at 1500 nm using a rate equations model and its value at room temperature is only  $3 \pm 1$  ps.

## I. INTRODUCTION

Tetravalent chromium ions ( $\text{Cr}^{4+}$ ) are active laser centers in forsterite ( $\text{Mg}_2\text{SiO}_4$ ),<sup>1</sup> YAG,<sup>2</sup> and  $\text{Y}_2\text{SiO}_5$ ,<sup>3</sup> where tunable stimulated emission has been observed in the near infrared between 1.1 and 1.6  $\mu\text{m}$  in the cw regime and at room temperature. In  $\text{Cr}^{4+}(\text{Cr})$ :forsterite the broad absorption bands that span in the visible from 500 to 790 nm ( ${}^3A_2-{}^3T_{1a}$  transition, see Fig. 1 based on Refs. 4 and 5) and in the infrared from 900 to 1140 nm ( ${}^3A_2-{}^3T_2$  transition) were used for excitation of stimulated emission with various lasers as pump sources. Although pumping directly to the  ${}^3T_2$  band near 1  $\mu\text{m}$  by Nd and Yb lasers or InGaAs laser diodes is more efficient because it is closer to the emission wavelength, excitation to the higher lying  ${}^3T_{1a}$  band due to the larger absorption cross section is attractive for direct diode pumping with InGaAlP semiconductor lasers<sup>6</sup> and for femtosecond pulse generation, because the use of short laser rods is beneficial both when applying large area non-diffraction limited pumping sources and when the higher order dispersion effects in the resonator have to be compensated.

The laser efficiency of  $\text{Cr}^{4+}$ -doped materials is in general lower than the efficiencies achievable with Ti sapphire or  $\text{Cr}^{3+}$  doped hosts. Recently, the excited state absorption (ESA) from the  ${}^3A''[{}^3E({}^3T_2)]$  storage state (see Fig. 1) was shown to be an important source of losses not only in the near infrared where the luminescence of the  $\text{Cr}^{4+}$  ion occurs,<sup>4</sup> but also at shorter wavelengths corresponding to the  ${}^3A_2-{}^3T_{1a}$  (Ref. 7) and  ${}^3A_2-{}^3T_2$  (Ref. 8) transitions used for pumping. In Cr:forsterite the stimulated amplification has been assigned to the  ${}^3A''[{}^3E({}^3T_2)]-{}^3A_2$  transition and the lack of emission from higher lying states suggests that the  $\text{Cr}^{4+}$  ions relax most of all nonradiatively from these states towards the metastable  ${}^3A''[{}^3E({}^3T_2)]$  state when excited directly from the ground state  ${}^3A_2$  or by ESA from  ${}^3A''[{}^3E({}^3T_2)]$ . The knowledge about the population dynamics following ESA, the nonradiative transitions as well as the energy transfer to  $\text{Cr}^{3+}$  ions that might be also present is crucial for understanding the loss mechanisms as factors that influence the laser performance of Cr:forsterite. Specifically

the decay rate from  ${}^3T_{1a}$  affects the probability for the excitation energy transfer to the  ${}^4T_2$  and  ${}^2E$  bands of the  $\text{Cr}^{3+}$  ion which was identified in EPR spectroscopical experiments as a loss mechanism.<sup>9</sup> Using up-converted luminescence and excited-state excitation spectroscopy the  ${}^3T_{1b}$  lifetime was measured in Ref. 10 to be 395 ps and the  ${}^3T_{1a}$  lifetime was estimated to be of the order of a few hundred nanoseconds, both at nitrogen temperature. The latter result obviously contradicts the laser experiment with ruby laser pumping<sup>11</sup> where excitation to the  ${}^3A''[{}^3E({}^3T_{1a})]$  state was used and the buildup time of the gain-switched Cr:forsterite laser did not exceed 5 ns. By measuring the rise time of the luminescence from the  ${}^3A''[{}^3E({}^3T_2)]$  state following excitation to  ${}^3T_{1a}$  by 20 ps pulses at the second harmonic of a Nd:YAlO<sub>3</sub> laser the  ${}^3T_{1a}$  excited state lifetime was estimated in Ref. 7 to be less than 5 ns (the temporal response of registration system) at room as well as at 77 K temperature. In Ref. 12 time resolved measurements of ESA with picosecond continuum provided an upper limit of 15 ps for the  ${}^3T_{1a}$  lifetime

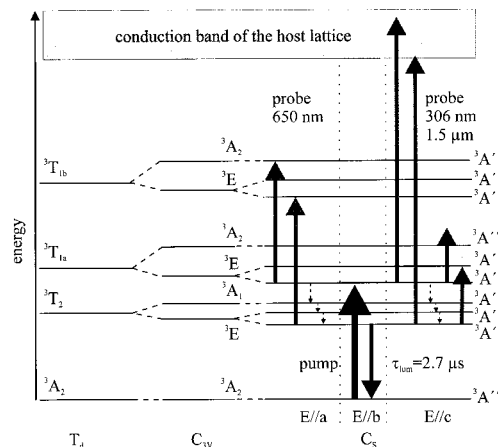


FIG. 1. Energy levels and excited state absorption transitions for  $\text{Cr}^{4+}$  in the site of  $T_d$ ,  $C_{3v}$ , and  $C_s$  symmetry based on Refs. 4 and 5. Singlet levels are omitted. The notations  ${}^3T_{1a}$  and  ${}^3T_{1b}$  correspond to the  ${}^3T_1(3F)$  and  ${}^3T_1(3P)$  states and are used for brevity.

at room temperature determined by the instrumental response.

Here, we present the results of  ${}^3T_{1a}$  lifetime measurements using two color pump and probe technique with femtosecond temporal resolution. For the first time to our knowledge the nonradiative relaxation from  ${}^3T_{1a}$  could be temporally resolved. The measured value of 3 ps reveals unexpectedly fast nonradiative relaxation which proceeds on the same time scale as the energy redistribution within the  ${}^3T_2$  manifold (an upper limit of 10 ps estimated in Ref. 13) and also within  ${}^3T_{1a}$  itself the latter being slowed down by the presence of an electronic bottleneck.<sup>14</sup>

## II. EXPERIMENT

The Cr:forsterite samples used in the present experiment were oriented and polished for propagation along the crystallographic  $a$  or  $c$  axes (Pbnm space group notation). They were grown by the Czochralski method and the concentration of  $\text{Cr}^{4+}$  ions determined from measurements of the absorption coefficient at 1064 nm was about  $1.05 \times 10^{19} \text{ cm}^{-3}$ . On one hand the sample thickness had to be chosen large enough in order to ensure sufficient absorption changes having in mind the restricted pump energy when using fs pulses and the principle limitation of the doping level in Cr:forsterite. On the other hand, the usable thickness was limited by Kerr type nonlinear effects induced by the pump pulse at the relatively high peak intensities of amplified fs pulses and also by the loss of temporal resolution caused by group velocity mismatch. We note that Sellmeier sets of dispersion equations for forsterite were not available in order to predict the group velocity mismatch between the pump and probe pulses.

We used pump pulses of 100 fs duration either from a fs Ti: sapphire regenerative amplifier at 773 nm or from the frequency doubled signal output of a traveling wave optical parametric generator at 750 nm which was pumped by the regenerative amplifier at 1 kHz repetition rate. Probe pulses of comparable duration were derived from the same optical parametrical generator using the fundamental, the second, and the fourth harmonic of the signal output. The wavelength of 773 nm was the minimum at which sufficient output power of the regenerative amplifier was available to pump the optical parametric generator. To generate a signal wavelength of 1500 nm as a probe, longer wavelengths of the regenerative amplifier had to be applied in order to move away from the degeneracy point of the optical parametric generator. Since the ground state absorption in this case was too low to induce sufficient population redistribution we used for this purpose the frequency doubled signal (750 nm) as a pump pulse. The exact value of the pump wavelength (773 or 750 nm) makes no qualitative difference for the temporal measurements presented but affects only the signal to noise ratio.

In all experiments the pump beam was linearly polarized along the sample  $b$  axis ( $E\parallel b$ ) and propagated along the  $a$  axis for  $E\parallel c$  probing and along the  $c$  axis for  $E\parallel a$  probing. Probe wavelengths of 306 nm ( $E\parallel c$ ), 650 nm ( $E\parallel a$ ), and 1500 nm ( $E\parallel c$ ) correspond to the maxima of the ESA bands observed previously in experiments with  $\mu\text{s}$  and ps temporal resolution.<sup>4,12</sup> The pump and probe pulses were focused by a

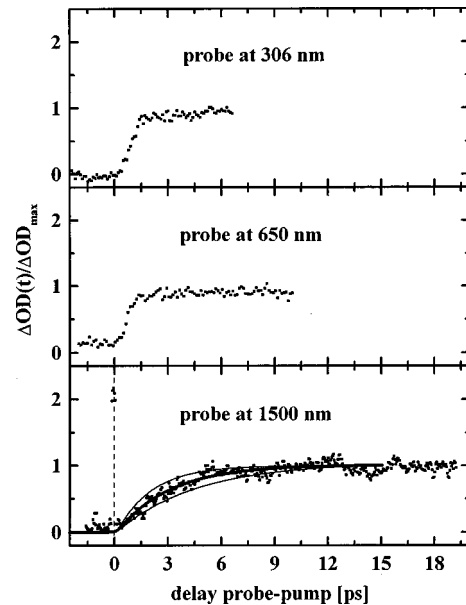


FIG. 2. Time evolution of the normalized optical density at 306, 650, and 1500 nm for a sample thickness of 1 mm. The solid curves for the case of 1500 nm probing are computer fits to the experimental data (solid squares) using the rate equations described in the text. The dashed line marks the zero position as determined by the artifact.

20-cm lens and traversed the samples collinearly. Great care was taken to ensure good spatial overlap between the beams. The difference in the transmission of the probe beam through the pumped and unpumped sample  $\Delta T$  was measured as a function of the pump-probe delay with lock-in-modulation and averaging technique. First we checked the sign of  $\Delta T$  by modulating the probe beam and interrupting the pump. For the pump and probe wavelengths given above the probe signal always had smaller values when the samples were pumped, which means that the pump induced additional losses at the probe wavelengths, i.e., depletion of the ground state absorption could be ruled out as an underlying mechanism for the pump induced absorption changes. In the actual measurement the pump beam was modulated and the probe beam was detected. The optical density variation  $\Delta OD$  was calculated then from the measured  $\Delta T$  values and normalized to its maximum value. All measurements were performed at room temperature.

## III. RESULTS AND DISCUSSION

The results of the femtosecond pump-and-probe measurements in Cr:forsterite showing the time evolution of the pump induced ESA at the probe wavelength are displayed in Fig. 2. The peak on-axis pump intensity was of the order of  $20 \text{ GW/cm}^2$  for probe wavelengths of 306 and 650 nm and  $100 \text{ GW/cm}^2$  for 1500 nm where the ESA cross section is smaller.<sup>4</sup> The salient features of the curves are a rapid rise followed by a plateau (a slow decay which exhibits no appreciable change over the time scale of our measurements). However, the rise times (time for growth of  $\Delta OD(t)/\Delta OD_{\text{max}}$  from 10 to 90%) derived from the experimental curves at 1-mm sample thickness were different for each probe wavelength. They amounted to about 800 fs, 1.1

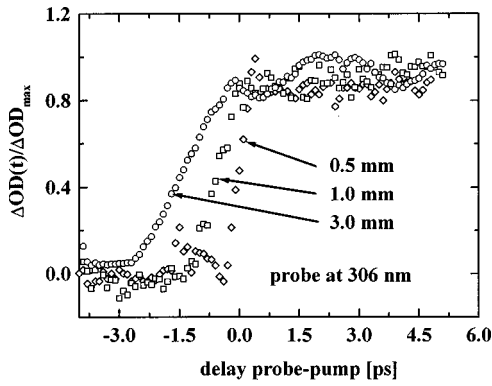


FIG. 3. Time evolution of the normalized optical density at 306 nm for samples with thickness of 0.5 mm (diamonds), 1.0 mm (squares), and 3.0 mm (circles). For this relative presentation the common zero of the abscissa was chosen to correspond to the zero point determined by difference frequency generation without any sample. Because of the larger group velocity of the pump pulse the transitions of all curves are shifted to negative delays.

ps, and 3.7 ps for wavelengths of 650, 306, and 1500 nm, respectively. Additional measurements were performed for samples of 0.5 and 3 mm thickness and quite different values of the rise time were obtained for 306 and 650 nm probing. Figure 3 shows these differences for the 306 nm probe wavelength, where they were more pronounced. To determine the group velocity mismatch between the pump and probe pulses we performed sum-frequency and difference frequency generation in a 1-mm thick BBO crystal (type-II interaction) once with the Cr:forsterite samples in the beam path and a second time without them. From the delay correction necessary for efficient frequency mixing in the BBO crystal we estimated a group delay of about 750 fs/mm for the 306 nm probing and about 180 fs/mm for the 650 nm probing. Obviously such values of the group delay deteriorate the temporal resolution in these two cases. In the case of 1500 nm probing the delay corrections necessary were much smaller than the pulse durations and could not be reliably measured, which means that the overall temporal resolution is determined by the cross correlation function FWHM (about 150 fs).

To analyze the experimental results the energy level diagram in Fig. 1 was used. The pump pulse at 773 or 750 nm ( $E||b$ ) populates the  ${}^3A''[{}^3E({}^3T_{1a})]$  state situated below the  ${}^3A''[{}^3A_2({}^3T_{1a})]-1E$  bottleneck.<sup>14</sup> This means that under our experimental conditions the bottleneck effect originating from state crossing should not be present. The  ${}^3A''[{}^3E({}^3T_{1a})]$  state is depopulated by nonradiative relaxation to the metastable  ${}^3T_2$  band located below. The strong polarization dependent ESA is assigned in the infrared (1100–2100 nm) to transitions from the  ${}^3A''[{}^3E({}^3T_2)]$  storage state to the  ${}^3A''[{}^3E({}^3T_{1a})]$  state for ( $E||c$ ), and in the visible (600–800 nm) to transitions from  ${}^3A''[{}^3E({}^3T_2)]$  to the  ${}^3A''[{}^3E({}^3T_{1b})]$  state for  $E||a$  where similar splitting (and selection rules) are assumed for  ${}^3T_{1b}$  as for the  ${}^3T_{1a}$  state.<sup>4</sup> In ground state absorption measurements the splitting of the  ${}^3T_{1b}$  state has not been identified yet, but an average value of 26 800  $\text{cm}^{-1}$  for its position was given in Ref. 15. In the UV (200–450 nm) strong ESA has been observed previously for all polarizations<sup>4</sup> that can be attributed to the transitions

from the same storage state to yet higher excited states or to the conduction band of the host lattice and to the charge transfer transitions. The exact position of the charge transfer state is unknown in Cr:forsterite but it can be assumed to be equal to that in  $\text{Cr}^{4+}:\text{Ca}_2\text{GeO}_4$  which has a similar structure [43 000  $\text{cm}^{-1}$  (Ref. 16)]. We note that at a pump wavelength of 306 nm the ESA cross section is more than an order of magnitude larger than the ground state absorption at this wavelength and at 1500 nm this ratio is even higher.<sup>4</sup> The ESA cross section at 650 nm is not known but the ground state absorption at this wavelength which is in part due to the  $\text{Cr}^{3+}$  ions present corresponds actually to a transition from  ${}^3A_2$  to  ${}^3E({}^3T_{1a})$  which is not optically allowed in  $\text{Cr}^{4+}$ .<sup>4,12</sup>

In our experiment the pulses at 306 nm probe the ESA transitions to the conduction band of the host lattice and the charge transfer transitions. The ESA at 306 nm, as can be seen in Fig. 2 has an instantaneous character. The photons at 306 nm have enough energy for transitions both from the directly pumped  ${}^3A''[{}^3E({}^3T_{1a})]$  state and from the  ${}^3A''[{}^3E({}^3T_2)]$  storage state (see Fig. 1) populated by the nonradiative relaxation. The measured ESA rise time corresponds in this case to the group velocity mismatch between the pump and probe pulses or equivalently to the instrumental response since equal probabilities could be assumed for the two transitions.

The ESA for probe pulses at 650 nm exhibits a similar instantaneous behavior. At longer delays we have ESA transitions from the  ${}^3A''[{}^3E({}^3T_2)]$  storage state to the lowest orbital component of the  ${}^3T_{1b}$  state. By adding our probe pulse energy (15 385  $\text{cm}^{-1}$ ) to the  ${}^3A''[{}^3E({}^3T_2)]$  energy [9150  $\text{cm}^{-1}$  (Ref. 14)] we obtain 24 535  $\text{cm}^{-1}$  which according to calculations should correspond to the  ${}^3A''[{}^3E({}^3T_{1b})]$  state.<sup>9</sup> The total excitation energy in our case (pump+probe) corresponds to 28 322  $\text{cm}^{-1}$  (12 937+15 385  $\text{cm}^{-1}$ ) which can be identified on the other hand with the location of a higher lying orbital component of the  ${}^3T_{1b}$  state. According to calculations<sup>9</sup> this should be the  ${}^3A''[{}^3A_2({}^3T_{1b})]$  state which is optically allowed for our probe wavelength at  $E||a$ . The presence of such higher lying state although not clearly seen in the ground state absorption spectra is confirmed by laser experiments with UV pumping.<sup>17,18</sup> Accordingly, just after absorption of the pump pulse excited state transitions from the directly pumped  ${}^3A''[{}^3E({}^3T_{1a})]$  state to the  ${}^3A''[{}^3A_2({}^3T_{1b})]$  state are possible. In the other channel from the  ${}^3A''[{}^3E({}^3T_2)]$  to the  ${}^3A''[{}^3E({}^3T_{1b})]$  state the ESA at 650 nm takes place during the nonradiative decay. Consequently the pulses at 650 nm probe the ESA at different delays first from the directly pumped  ${}^3A''[{}^3E({}^3T_{1a})]$  state and then from the populated by nonradiative transitions  ${}^3A''[{}^3E({}^3T_2)]$  storage state. Temporal resolution of the nonradiative decay is possible in this case if only the probabilities for the two transitions are quite different. Taking into account, however, the dependence of the rise times measured at the probe wavelength of 650 nm with crystals of different thickness we conclude that these probabilities are similar and the measured rise time should be attributed to the instrumental response. We note that the actual rise time of the ESA in this measurement is related to the directly pumped  ${}^3A''[{}^3E({}^3T_{1a})]$  state and not to the  ${}^3A''[{}^3E({}^3T_2)]$  storage state as in Ref. 12.

Using, however, probe pulses near 1500 nm it is impos-

sible to reach the  ${}^3T_{1b}$  band from the directly pumped  ${}^3A''[{}^3E({}^3T_{1a})]$  state and ESA occurs only due to the  ${}^3A''[{}^3E({}^3T_2)]-{}^3A''[{}^3E({}^3T_{1a})]$  transition (see Fig. 1). In this case the rise time of the ESA corresponds to the relaxation time from  ${}^3A''[{}^3E({}^3T_{1a})]$  to  ${}^3T_2$ . The underlying assumption here is that the 1500 nm pulse interrogates the relaxed to  ${}^3A''[{}^3E({}^3T_2)]$  ions by an allowed transition for  $E\parallel c$ . Intraband relaxation within  ${}^3T_2$  is, however, included in the measured rise time. The pump-probe measurements performed with the samples of different thickness resulted in the same estimation for the rise time. Consequently we conclude that the temporal evolution of the normalized optical density difference as shown in Fig. 2 is not affected by group velocity mismatch. The artifact at 0-time delay was identified as induced focusing which modified the spatial distribution of the probe beam on the detector. It is more pronounced in the case of 1500 nm probing due to the increased pump intensity and served as a method to determine exactly the 0-delay point and to confirm the temporal resolution since the  $n_2$  effect can be regarded as instantaneous. Obviously the temporal resolution for 1500 nm probing is better than 200 fs in Fig. 2.

In order to obtain more detailed understanding of the experimental results, as well as to extract the nonradiative relaxation time from the  ${}^3A''[{}^3E({}^3T_{1a})]$  state to the  ${}^3A''[{}^3E({}^3T_2)]$  state we simulated the measurement using the following model for the excited-state transition dynamics at the probe wavelength of 1500 nm: the state that is optically excited is  ${}^3A''[{}^3E({}^3T_{1a})]$  (and not one mixed with the  ${}^1E$  singlet state), the ESA of the pump beam is ignored, the metastable storage state  ${}^3A''[{}^3E({}^3T_2)]$  is populated through nonradiative relaxation, and also here the singlet levels are omitted in the ESA analysis. The population kinetics of the ground state  ${}^3A_2$ , and the  ${}^3A''[{}^3E({}^3T_{1a})]$  and  ${}^3A''[{}^3E({}^3T_2)]$  states involved in the ESA process is governed then by the following rate equations:

$$\frac{dN_0}{dt} = -\frac{\sigma_{\text{GSA}}}{h\nu} I_p(t) N_0, \quad (1)$$

$$\frac{dN_2}{dt} = \frac{\sigma_{\text{GSA}}}{h\nu} I_p(t) N_0 - \frac{N_2}{\tau_{21}}, \quad (2)$$

$$\frac{dN_1}{dt} = \frac{N_2}{\tau_{21}}, \quad (3)$$

where  $N_0(t)$ ,  $N_2(t)$ , and  $N_1(t)$  denote the instantaneous population densities of  ${}^3A_2$ ,  ${}^3A''[{}^3E({}^3T_{1a})]$ , and  ${}^3A''[{}^3E({}^3T_2)]$ , respectively,  $I_p(t)$  is the pump pulse intensity,  $\tau_{21}$  is the nonradiative relaxation time of the  ${}^3A''[{}^3E({}^3T_{1a})]$  state, and  $\sigma_{\text{GSA}} = 2.5 \times 10^{-18} \text{ cm}^2$  (Ref. 7) is the ground-state absorption cross section at the pump wavelength. The rate equations were solved numerically using a fourth-order Runge-Kutta method with initial values  $N_0 = N$ ,  $N_2 = N_1 = 0$ , where  $N$  is the total number of active ions.

The pump pulse is assumed to be Gaussian in time with a cross section larger than the cross section of the probe beam. The change in the optical absorption of the probe pulse at a particular delay time  $t_d$  is calculated in terms of  $N_1(t)$  by

$$OD(t_d) = -\ln \left[ \frac{\int_{-\infty}^{+\infty} I_{\text{pr}}(t-t_d) \exp[-\sigma_{\text{ESA}} N_1(t)L] dt}{\int_{-\infty}^{+\infty} I_{\text{pr}}(t) dt} \right] \quad (4)$$

and normalized to the maximal value corresponding to the one approached at maximum delay time. Here  $I_{\text{pr}}(t)$  is the probe pulse intensity profile approximated as Gaussian with a FWHM of 100 fs,  $L$  is the sample length, and  $\sigma_{\text{ESA}}(1500 \text{ nm}) = 9.5 \times 10^{-19} \text{ cm}^2$  is the ESA cross section at 1500 nm.<sup>4</sup>

The best fit to the experimental data is shown in Fig. 2 (probe at 1500 nm) with a thick solid line and corresponds to a  ${}^3A''[{}^3E({}^3T_{1a})]$  state lifetime of 3 ps whereas the two thin lines correspond to  $\pm 1$  ps deviation from that estimation. The plateau region in all measured ESA curves at long delays reflects the depopulation of the  ${}^3A''[{}^3E({}^3T_2)]$  storage state which occurs predominantly by radiative transitions with a luminescence lifetime of 2.7  $\mu\text{s}$  at room temperature.<sup>14</sup>

#### IV. CONCLUSION

In conclusion we performed time resolved pump and probe measurements of ESA in Cr:forsterite with femtosecond resolution and the results were fitted using rate equations. The salient features of the normalized optical density curves are a rapid rise time followed by a slow decay. From the rise time the nonradiative transition from  ${}^3T_{1a}$  to the  ${}^3T_2$  metastable band could be temporally resolved for the first time yielding 3 ps at room temperature, and the long decay of the curves observed reflects the radiative depopulation of the metastable  ${}^3T_2$  band ( $\approx 3 \mu\text{s}$ ). The fast relaxation measured here from the  ${}^3A''[{}^3E({}^3T_{1a})]$  state indicates that the estimations of the intraband thermalization within the  ${}^3T_2$  manifold<sup>13</sup> should be revised. In the present work this could not be done because of the limited absorption of the samples for direct  ${}^3A_2-{}^3T_2$  excitation. The fast nonradiative depopulation of the  ${}^3T_{1a}$  band observed by us supports and explains the conclusion that the energy transfer to  $\text{Cr}^{3+}$  ions from this band is less probable than intracenter nonradiative decay drawn in Ref. 19 on the basis of missing luminescence from the  ${}^4T_2$  band in  $\text{Cr}^{3+}$ . Nevertheless the concentration of  $\text{Cr}^{3+}$  ions should be kept low when pumping Cr:forsterite lasers near 750 nm (Ref. 6) because of the possibility for direct absorption of the pump radiation.

#### ACKNOWLEDGMENT

We acknowledge financial support by the Federal Ministry of Education, Science, Research and Technology (BMBF, Germany) under Contract No. 13N7214/3.

\*Author to whom correspondence should be addressed. FAX: +49-30-6392 1289. Electronic address: petrov@mbi-berlin.de

<sup>1</sup>V. Petricevic, S. K. Gayen, and R. R. Alfano, Appl. Phys. Lett. **53**, 2590 (1988).

<sup>2</sup>N. I. Borodin, V. A. Zhitnyuk, A. G. Okhrimchuk, and A. V. Shestakov, Izv. Akad. Nauk SSSR, Ser. Fiz. **54**, 1500 (1990) [Bull. Acad. Sci. USSR, Phys. Ser. **54**, 54 (1990)].

<sup>3</sup>J. Koetke, S. Kück, K. Petermann, G. Huber, G. Cerullo, M.

- Danailov, V. Magni, L. F. Qian, and O. Zvelto, *Opt. Commun.* **101**, 195 (1993).
- <sup>4</sup>N. V. Kuleshov, V. G. Shcherbitsky, V. P. Mikhailov, S. Hartung, T. Danger, S. Kück, K. Petermann, and G. Huber, *J. Lumin.* **75**, 319 (1997).
- <sup>5</sup>W. Jia, H. Liu, S. Jaffe, W. M. Yen, and B. Denker, *Phys. Rev. B* **43**, 5234 (1991).
- <sup>6</sup>L. Qian, X. Liu, and F. Wise, *Opt. Lett.* **22**, 1707 (1997); X. Liu, L. Qian, F. Wise, Z. Zhang, T. Itatani, T. Sugaya, T. Nakagawa, and K. Torizuka, *Appl. Opt.* **37**, 7080 (1998).
- <sup>7</sup>V. P. Mikhailov, N. I. Zhavoronkov, N. V. Kuleshov, A. S. Avtukh, and V. G. Shcherbitsky, *Opt. Quantum Electron.* **27**, 767 (1995).
- <sup>8</sup>A. S. Avtukh, N. I. Zhavoronkov, and V. P. Mikhailov, *Opt. Spektrosk.* **83**, 483 (1997) [*Opt. Spectrosc.* **83**, 451 (1997)].
- <sup>9</sup>V. G. Baryshevski, M. V. Korzhik, M. G. Livshitz, A. A. Tarasov, A. E. Kimaev, I. I. Mishkel, M. L. Meilman, B. J. Minkov, and A. P. Shkadarevich, in *OSA Proceedings on Advanced Solid-State Lasers, 1991*, edited by G. Dube and L. Chase (OSA, Washington, DC, 1991), Vol. 10, pp. 26–34.
- <sup>10</sup>S. G. Demos, V. Petricevic, and R. R. Alfano, *Phys. Rev. B* **52**, 1544 (1995).
- <sup>11</sup>I. T. McKinnie, L. A. W. Gloster, T. A. King, and R. T. White, *Appl. Opt.* **36**, 4985 (1997).
- <sup>12</sup>K. V. Yumashev, N. V. Kuleshov, P. V. Prokoshin, A. M. Malyrevich, and V. P. Mikhailov, *Appl. Phys. Lett.* **70**, 2523 (1997).
- <sup>13</sup>A. Seas, V. Petricevic, and R. R. Alfano, in *OSA Proceedings on Advanced Solid-State Lasers* (Ref. 9), pp. 57–59.
- <sup>14</sup>S. G. Demos and R. R. Alfano, *Phys. Rev. B* **52**, 987 (1995); D. M. Calistru, S. G. Demos, and R. R. Alfano, *Phys. Rev. Lett.* **78**, 374 (1997).
- <sup>15</sup>V. Petricevic, S. K. Gayen, and R. R. Alfano, in *OSA Proceedings on Tunable Solid State Lasers, 1989*, edited by M. L. Shand and H. P. Jenssen (OSA, Woodbury, NY, 1989), Vol. 5, pp. 77–84.
- <sup>16</sup>M. F. Hazenkamp, H. U. Güdel, M. Atanasov, U. Kesper, and D. Reinen, *Phys. Rev. B* **53**, 2367 (1996).
- <sup>17</sup>V. G. Baryshevskii, V. A. Voloshin, S. A. Demidovich, A. E. Kimaev, M. V. Korzhik, M. G. Livshits, M. L. Meil'man, B. I. Minkov, and A. P. Shkadarevich, *Kvant. Elektr. (Moscow)* **17**, 1389 (1990) [*Sov. J. Quantum Electron.* **20**, 1297 (1991)].
- <sup>18</sup>I. T. McKinnie, *J. Mod. Opt.* **43**, 1753 (1996).
- <sup>19</sup>H. R. Verdun and L. Merkle, in *OSA Proceedings on Advanced Solid-State Lasers* (Ref. 9), pp. 35–40.